

Idiopathic neutropenia with fewer than 5% dysplasia may be a distinct entity of idiopathic cytopenia of undetermined significance

Keiko Ando · Atsushi Kodama · Tamiko Iwabuchi ·
Junko H. Ohyashiki · Kazuma Ohyashiki

Received: 21 September 2009 / Accepted: 28 September 2009
© Springer-Verlag 2009

Dear Editor,

A condition marked by fewer than 10% of dysplastic cells and fewer than 5% of blasts in the bone marrow (BM) is now categorized as idiopathic cytopenia of undetermined significance (ICUS); if clonal cytogenetic changes are detectable in ICUS patients, the diagnosis can be changed to myelodysplastic syndrome (MDS) [1]. This categorization is very practical and clear-cut in separating MDS from those with low-grade dysplasia [1], and it thus became possible to analyze the clinical and hematologic features to differentiate refractory cytopenia with unilineage dysplasia (RCUD) from ICUS. However, only a single report dealing with possible ICUS with dysplastic features in each cell lineage appears to exist, that by Wimazal et al. [2]. We therefore focused on cytopenia patients with fewer than 5% of BM blasts and reassessed the dysplastic features, in combination with the cytogenetic results, to shed light on low-grade dysplasia.

Electronic supplementary material The online version of this article (doi:10.1007/s00277-009-0845-0) contains supplementary material, which is available to authorized users.

K. Ando · T. Iwabuchi · K. Ohyashiki (✉)
The First Department of Internal Medicine (Hematology
Division), Tokyo Medical University,
6-7-1 Nishishinjuku, Shinjuku-ku,
Tokyo 160-0023, Japan
e-mail: ohyashik@r.ij4u.or.jp

A. Kodama
Division of Cytogenetics, Central Laboratory,
Tokyo Medical University,
Tokyo, Japan

J. H. Ohyashiki
Intractable Disease Research Center, Tokyo Medical University,
Tokyo, Japan

From 1994 to 2008, we performed BM examinations with cytogenetic studies in 445 patients with cytopenia, 237 of whom were given diagnoses of MDS or suspected MDS. As well as we could, we used the initial BM examination to rule out the possibility of other underlying disorders inducing cytopenia, and as a result, 137 patients with fewer than 5% marrow blasts were enrolled in this study. Of these 137 patients, 56 who were followed for more than 6 months and for whom specimens were available for reanalyzable marrow films (200 cells being examined in each cell lineage) were used in this study [3, 4]; two patients with hypoplastic BM without cytogenetic changes were excluded from this study since we could not completely rule out the possibility of low-grade aplastic anemia.

In this study, we reassessed the bone marrow films for 16 patients with ICUS (Electronic supplementary materials, File 1), 16 with RCUD (Electronic supplementary materials, File 2), and 22 patients with refractory cytopenia with multilineage dysplasia (RCMD; Electronic supplementary materials, File 3). No particular difference in the peripheral blood data was found among patients with ICUS, RCUD, and RCMD. RCUD patients had more dysgranulopoietic cells than those with ICUS ($16.7 \pm 19.4\%$ vs $3.5 \pm 3.3\%$, $P=0.0116$) because of the presence of hypogranular neutrophils or pseudo-Pelger anomaly, while no significant difference in percentages of dyserythropoietic cells was noted ($P=0.1809$; Electronic supplementary materials, File 4). This indicates that ICUS patients can usually be diagnosed from the absence of prominent dysgranulopoiesis.

We then separated the ICUS patients into two groups according to the percentages of dysplastic cells (Table 1). ICUS patients with fewer than 5% dysplastic cells in at least one cell lineage had a significantly lower absolute neutrophil count than those with 5% to 9% of dysplastic

Table 1 Hematologic parameters of patients with idiopathic cytopenia of undetermined significance classified by percentages of dysplastic cells

	ICUS (<5% dysplasia)	ICUS (5–9% dysplasia)	<i>P</i> value
No. of patients	7	9	
Age (years)	55.6±14.9	53.0±20.7	0.7861
Leukocytes ($\times 10^6/L$)	2,586±647	3,533±1,587	0.1616
Neutrophils ($\times 10^6/L$)	1,086±296	2,308±1,305	0.0302
Lymphocytes ($\times 10^6/L$)	1,273±421	1,016±310	0.1815
Monocytes ($\times 10^6/L$)	117±53	184±137	0.2429
Hb (g/dL)	12.4±1.9	11.4±3.4	0.5172
Platelets ($\times 10^9/L$)	197±78	111±94	0.071
MCV (fL)	94.8±5.8	98.6±15.0	0.5386
Marrow blasts (%)	1.6±0.6	1.9±1.2	0.5864
Dyserythropoiesis (%)	1.4±1.1	3.4±2.8	0.0994
Dysgranulopoiesis (%)	1.4±1.2	5.1±3.5	0.0176
Cytogenetics			
Normal karyotypes	7	6	
Non-clonal changes	0	0	
Clonal changes	0	3 (2*)	

Hb hemoglobin, MCV mean corpuscular volume, 2* two patients showed a clonal missing Y chromosome

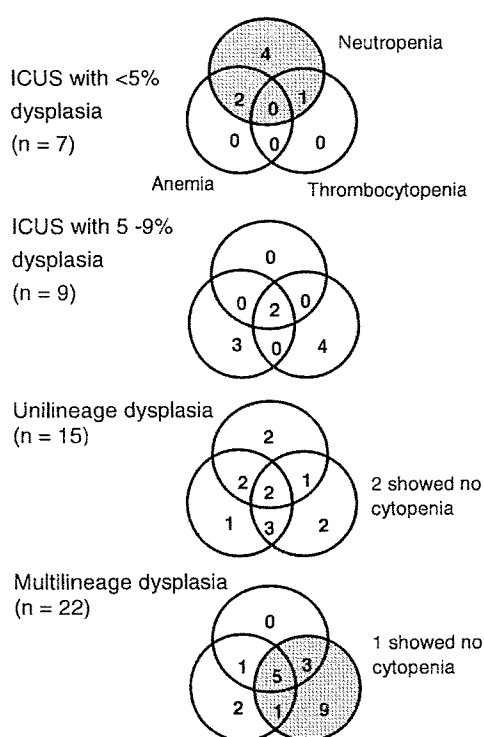


Fig. 1 Diagram of cytopenia pattern in patients showing fewer than 5% of marrow blasts. Overlapping portions show cytopenia in two cell lineages (bi-cytopenia), and the central overlapping portion indicates pancytopenia. Note the cytopenic pattern in the ICUS patients with <5% dysplasia (*top*) who show predominant neutropenia. One RARS patient with unilineage dysplasia is excluded from this diagram. We utilized the definition of the Working Conference on MDS for cytopenia [4]; neutropenia for less than $1,500 \times 10^6/L$, hemoglobin for less than 11 g/dL, and thrombocytopenia for less than $100 \times 10^9/L$

cells ($1,086 \pm 296 \times 10^6/L$ vs $2,308 \pm 1,305 \times 10^6/L$; $P=0.0302$), while the leukocyte counts did not differ significantly: $2,586 \pm 647 \times 10^6/L$ vs $3,533 \pm 1,587 \times 10^6/L$ ($P=0.1616$). The pattern of cytopenia in the ICUS patients with fewer than 5% dysplastic cells showed prominent neutropenia (less than $1,500 \times 10^6/L$; Fig. 1). Chromosome changes were detected in only three patients with ICUS with 5% to 9% of dysplastic cells: One showed non-clonal del(20q) and -Y, one, -Y, and one clonal del(20q). None of them developed MDS or aplastic anemia during a mean follow-up period of 42.25 months.

The current observation indicates that ICUS patients may be heterogeneous and that the group with fewer dysplastic cells with no detectable cytogenetic changes preferentially exhibited neutropenia (Fig. 1), and so the etiology of patients in this group may be different from the ICUS patients with more dysplastic cells (5% to 9%). Another point that was noticed is that all three patients (two with ICUS morphology and one with RCUD) with del(20q), whether they had a clonal nature or not, consistently exhibited thrombocytopenia alone and were clustered in the low blast percentage and low dysplastic cell frequency group. This suggests that the detection of cells with del(20q), using fluorescence in situ hybridization analysis, in low-grade MDS, including morphologically identified ICUS [5], might be important in MDS diagnosis since the detection of cytogenetic changes is important in the diagnosis of MDS.

Acknowledgments Thanks are due to Professor J Patrick Barron, of the International Medical Communication Center of Tokyo Medical University, for his review of this manuscript. AK, TI, and KO

performed hematologic examination, AK did cytogenetic study, and JHO reviewed the paper.

Conflict of interest None.

References

1. Brunning RD, Orazi A, Germing U, Le Beau MM, Porwit A, Vardiman JW et al (2008) Myelodysplastic syndromes. In: Swerdlow SH, Campo E, Harris NL, Jaffe ES, Pileri SA, Stein H, Thiele J, Vardiman JW (eds) WHO classification of tumours of hematopoietic and lymphoid tissues. IARC, Lyon, pp 90–107
2. Wimazal F, Fonatsch C, Thalhammer R, Schwarzinger I, Müllauer L, Sperr WR et al (2007) Idiopathic cytopenia of undetermined significance (ICUS) versus low risk MDS: the diagnostic interface. *Leuk Res* 31:1461–1468
3. Mufti GJ, Bennett JM, Goasguen J, Bain BJ, Baumann I, Brunning R. International Working Group on Morphology of Myelodysplastic Syndrome et al (2008) Diagnosis and classification of myelodysplastic syndrome: International Working Group on Morphology of myelodysplastic syndrome (IWGM-MDS) consensus proposals for the definition and enumeration of myeloblasts and ring sideroblasts. *Haematologica* 93:1712–1717
4. Valent P, Horney H-P, Bennett JM, Fonatsch C, Germing U, Greenberg P et al (2007) Definitions and standards in the diagnosis and treatment of the myelodysplastic syndromes: consensus statements and report from a working conference. *Leuk Res* 31:727–736
5. Gupta R, Soupir CP, Johari V, Hasserjian RP (2007) Myelodysplastic syndrome with isolated deletion of chromosome 20q: an indolent disease with minimal morphological dysplasia and frequent thrombocytopenic presentation. *Br J Haematol* 139:265–288

ORIGINAL ARTICLE

Identification of *Zfp521/ZNF521* as a cooperative gene for *E2A-HLF* to develop acute B-lineage leukemia

N Yamasaki¹, K Miyazaki¹, A Nagamachi², R Koller³, H Oda⁴, M Miyazaki⁵, T Sasaki¹, Z-i Honda⁶, L Wolff³, T Inaba² and H Honda¹

¹Department of Developmental Biology, Research Institute for Radiation Biology and Medicine, Hiroshima University, Minami-ku, Hiroshima, Japan; ²Department of Molecular Oncology, Research Institute for Radiation Biology and Medicine, Hiroshima University, Minami-ku, Hiroshima, Japan; ³Leukemogenesis Section, Laboratory of Cellular Oncology, National Cancer Institute, NIH, Bethesda, MD, USA; ⁴Department of Pathology, Tokyo Women's Medical University, Shinjuku-ku, Tokyo, Japan; ⁵Department of Immunology, Graduate School of Biomedical Sciences, Hiroshima University, Minami-ku, Hiroshima, Japan and ⁶Department of Allergy and Rheumatology, Faculty of Medicine, Graduate School of Medicine, University of Tokyo, Bunkyo-ku, Tokyo, Japan

E2A-hepatic leukemia factor (HLF) is a chimeric protein found in B-lineage acute lymphoblastic leukemia (ALL) with t(17;19). To analyze the leukemogenic process and to create model mice for t(17;19)-positive leukemia, we generated inducible knock-in (iKI) mice for *E2A-HLF*. Despite the induced expression of *E2A-HLF* in the hematopoietic tissues, no disease was developed during the long observation period, indicating that additional gene alterations are required to develop leukemia. To elucidate this process, *E2A-HLF* iKI and control littermates were subjected to retroviral insertional mutagenesis. Virus infection induced acute leukemias in *E2A-HLF* iKI mice with higher morbidity and mortality than in control mice. Inverse PCR detected three common integration sites specific for *E2A-HLF* iKI leukemic mice, which induced overexpression of zinc-finger transcription factors: *growth factor independent 1 (Gfi1)*, *zinc-finger protein subfamily 1A1 isoform a (Zfp1a1)*, also known as *Ikaros* and *zinc-finger protein 521 (Zfp521)*. Interestingly, tumors with *Zfp521* integration exclusively showed B-lineage ALL, which corresponds to the phenotype of human t(17;19)-positive leukemia. In addition, *ZNF521* (human counterpart of *Zfp521*) was found to be overexpressed in human leukemic cell lines harboring t(17;19). Moreover, both iKI for *E2A-HLF* and transgenic for *Zfp521* mice frequently developed B-lineage ALL. These results indicate that a set of transcription factors promote leukemic transformation of *E2A-HLF*-expressing hematopoietic progenitors and suggest that aberrant expression of *Zfp521/ZNF521* may be clinically relevant to t(17;19)-positive B-lineage ALL.

Oncogene advance online publication, 11 January 2010; doi:10.1038/onc.2009.475

Keywords: *E2A-HLF*; inducible knock-in mice; retrovirus insertional mutagenesis; *Zfp521/ZNF521*

Introduction

The *E2A* gene, which encodes a basic helix-loop-helix transcription factor of E-box DNA-binding proteins on chromosome 19, is the target of subsets of B-lineage acute lymphoblastic leukemia (ALL) (Look, 1997). As a result of the t(17;19)(q22;p13), the *E2A* gene is fused to the *HLF* gene on chromosome 17 (Inaba *et al.*, 1992). In the *E2A-HLF* chimeric gene product, the transactivation domain of *E2A* is fused to the basic region/leucine zipper domain of hepatic leukemia factor (HLF), which contributes to the DNA binding and dimerization (Inaba *et al.*, 1992). Clinically, ALL with the *E2A-HLF* chimera is refractory to intensive therapy and is frequently associated with coagulopathy and hypercalcemia (Hunger, 1996).

The biological properties of *E2A-HLF* were initially analyzed using cultured cells. We showed that the expression of *E2A-HLF* in NIH 3T3 cells induced anchorage-independent cell growth in soft agar and rendered these cells tumorigenic in nude mice (Yoshihara *et al.*, 1995; Inukai *et al.*, 1997). In addition, using a zinc-inducible system, we showed that *E2A-HLF* expression protects interleukin 3-dependent hematopoietic cells from interleukin 3 deprivation-induced apoptosis (Inaba *et al.*, 1996). Moreover, by a representational difference analysis, several downstream candidate genes of *E2A-HLF* were cloned, such as *annexin II* (Matsunaga *et al.*, 2003), *annexin VIII* and *sushi-repeat protein upregulated in leukemia (SRPUL)* (Kurosawa *et al.*, 1999), two *Groucho*-related genes, *Grg2* and *Grg6* (Dang *et al.*, 2001), and a gene encoding a zinc-finger transcription factor, *Slug* (Inukai *et al.*, 1999).

The *in vivo* roles of *E2A-HLF* were analyzed by transgenic and bone marrow transplantation studies. We and others generated transgenic mice expressing *E2A-HLF* under the control of lymphoid-specific promoters (Honda *et al.*, 1999; Smith *et al.*, 1999). The transgenic mice showed increased thymocyte apoptosis, B-cell maturation arrest and eventual development of ALL, mainly with T-cell phenotype (Honda *et al.*, 1999; Smith *et al.*, 1999). On the other hand, bone marrow (BM) B-cell progenitors retrovirally co-transduced

Correspondence: Dr H Honda, Department of Developmental Biology, Research Institute for Radiation Biology and Medicine, 1-2-3, Kasumi, Minami-ku, Hiroshima 734-8553, Japan.
E-mail: hhonda@hiroshima-u.ac.jp
Received 5 May 2009; revised 16 July 2009; accepted 23 November 2009

with *E2A-HLF* and *Bcl-2* produced immortalized cells, which developed leukemia when transplanted into syngeneic recipients (Smith *et al.*, 2002). These results showed that the expression of *E2A-HLF* perturbed normal lymphocyte development, rendered lymphocytes susceptible to malignant transformation and finally developed ALL. Interestingly, the phenotypes of the *E2A-HLF* transgenic mice closely resembled those of *E2A*-deficient mice, which also showed abnormal T-cell development, absence of B-cell precursors and rapid development of T-cell lymphomas (Bain *et al.*, 1994, 1997; Zhuang *et al.*, 1994). These results strongly suggested that *E2A-HLF* contributes to leukemogenesis by activating downstream target genes and/or by suppressing transcriptional activity of endogenous genes in a dominant-negative manner (Aspland *et al.*, 2001; Seidel and Look, 2001).

We showed the *in vivo* oncogenicity of *E2A-HLF* by a transgenic approach (Honda *et al.*, 1999). However, the transgenic system fundamentally differs from human disease in several ways. First, in the transgenic system, every cell contains the transgene and there are no normal cells, whereas the human disease originates from acquiredly transformed cells. Second, in the transgenic system, as the transgene-derived product is congenitally expressed, transgene-expressing cells are not eliminated by the immune system. In contrast, in human diseases, most transformed cells are ablated by immunocompetent cell and those that escape from this system proliferate and show a fully malignant phenotype. Therefore, the precise molecular mechanism(s) through which *E2A-HLF* contributes a growth advantage to hematopoietic cells and develops leukemia *in vivo* remains to be clarified.

In this study we report the generation and analysis of knock-in mice for *E2A-HLF* in which *E2A-HLF* was inducibly expressed under the control of the native regulatory elements of the *E2A* gene. Despite the induced *E2A-HLF* expression in the hematopoietic tissues, no disease was developed during the long-term observation period, indicating that secondary events are required for the development of leukemia. To elucidate this process, we applied retroviral insertional mutagenesis (RIM) using Moloney murine leukemia virus (MMLV), isolated common viral integration sites specific for *E2A-HLF*-expressing tumors, and identified Zfp521/ZNF521 as a cooperative gene for *E2A-HLF* to develop B-lineage ALL.

Results

Generation of inducible knock-in (iKI) mice for *E2A-HLF* and acquired expression of *E2A-HLF* in the hematopoietic tissues

To study the role of *E2A-HLF* in model animal systems that mimic human leukemogenesis, we planned to generate mice in which *E2A-HLF* could be inducibly expressed under the control of the native *E2A* promoter. For this purpose, we designed a knock-in vector in

which a genomic region of the *E2A* gene (a 3' part of exon 2, intron 2 and a 5' part of exon 3) was replaced by a cassette containing the *floxed neomycin* resistance (*Neo*) gene, followed by *E2A-HLF* complementary DNA, *IRES-GFP (IG)* and an *SV40 polyA* signal (*pA*) (Figure 1a). Embryonic stem cell clones with homologous recombination were identified by Southern blot analysis (Figure 1b, upper panel) using a 5' probe (Figure 1a) and by long-distance genomic PCR (Figure 1b, lower panel) using a 3' primer set (*P1* and *P2*, Figure 1a) and were used to create chimeric mice, which transmitted the mutant allele to the progeny and produced heterozygous mice (*EHKI^{Neo+}*). In the *EHKI^{Neo+}* mice, the expression of the knock-in allele-derived message was detected by reverse transcriptase-PCR (RT-PCR) using a primer set, *E2A-77* (derived from exon 1 of the *E2A* gene) and *HLF-2* (derived from the *HLF* portion of the *E2A-HLF* fusion complementary DNA) (Figure 1a) in all tissues examined (indicated by *Neo+* in Figure 1c, upper panel). However, because this message contains a *floxed Neo* gene and multiple in-frame stop codons, the *E2A-HLF* fusion protein cannot be translated. To confirm this, proteins extracted from tissues were immunoprecipitated with an anti-*E2A* antibody and immunoprecipitants were blotted with an anti-*HLF* antibody. As expected, no *E2A-HLF* protein (molecular weight 62 kDa) was detected in the hematopoietic tissues, such as the thymus or spleen of *EHKI^{Neo+}* mice (the first and fourth lanes in Figure 1d).

We then mated *EHKI^{Neo+}* mice with *MxCre* transgenic mice that express *Cre* under the control of the interferon-responsive *Mx* promoter (Kuhn *et al.*, 1995). *EHKI^{Neo+}/MxCre* compound mice were injected with polyinosinic/polycytidylic acid (pIpC), which is a strong and transient inducer of interferon, to delete the *floxed Neo* gene from the knocked-in allele and to create *Neo*-deleted (*EHKI^{ΔNeo}*) mice (Figure 1a). In the pIpC-treated *EHKI^{Neo+}/MxCre* (that is, *EHKI^{ΔNeo}*) mice, a shorter message was amplified in various tissues, including the thymus, heart, liver and spleen, by RT-PCR using *E2A-77* and *HLF-2* primers (indicated by Δ *Neo* in Figure 1c, lower panel), indicating that the *Neo* gene was successfully deleted in these tissues. As a result, the induced expression of *E2A-HLF* protein was achieved, as shown by immunoprecipitation/western blot analysis in the thymus and spleen of the *EHKI^{ΔNeo}* mice (the second and fifth lanes in Figure 1d).

MMLV infection induced acute leukemias in *EHKI^{ΔNeo}* mice at a higher frequency and with a shorter latency than in *EHKI^{Neo+}* mice

EHKI^{Neo+} and *EHKI^{Neo+}/MxCre* mice treated with pIpC were continuously observed for any sign of illness, including routine examination of peripheral blood parameters. However, during the long-term observation period, no abnormality was detected in *EHKI^{Neo+}* or *EHKI^{ΔNeo}* mice (Figure 2a, thin dotted and thin continuous lines). These results indicated that the induced *E2A-HLF* expression alone is not sufficient

and additional genetic changes are required for the development of leukemia.

To address this possibility, mice were subjected to retroviral insertional mutagenesis. Neonatal *EHKI^{Neo+}* and *EHKI^{Neo+}/MxCre* mice were infected with MMLV and were then injected with pIpC. Both types of mice developed leukemias, but MMLV-infected *EHKI^{ΔNeo}* (*EHKI^{ΔNeo}/MMLV*) mice showed higher morbidity and mortality than virus-infected *EHKI^{Neo+}* (*EHKI^{Neo+}/MMLV*) littermates (Figure 2a, thick dotted and thick continuous lines). *EHKI^{ΔNeo}/MMLV* mice began to develop acute leukemias at as early as 2.6 months of age, and all died by 6 months of age. In contrast, *EHKI^{Neo+}/MMLV* mice developed leukemias at approximately 4–6 months of age and 6 out of 11 mice died within 1 year. The difference in the survival curves

between *EHKI^{ΔNeo}/MMLV* and *EHKI^{Neo+}/MMLV* mice was statistically significant ($P < 0.01$).

***EHKI^{Neo+}/MMLV* mice mainly developed T-cell leukemia but *EHKI^{ΔNeo}/MMLV* mice showed B-progenitor and lineage marker-negative leukemias**

The leukemic mice were hematologically and macroscopically examined, and the leukemic cells were immunophenotypically and molecularly analyzed. Interestingly, macroscopic appearances of *EHKI^{Neo+}/MMLV* leukemic mice were different from those of *EHKI^{ΔNeo}/MMLV* leukemic mice.

Most of *EHKI^{Neo+}/MMLV* leukemic mice (four of six samples) showed thymic enlargement, associated with splenomegaly and lymph node swelling, except two

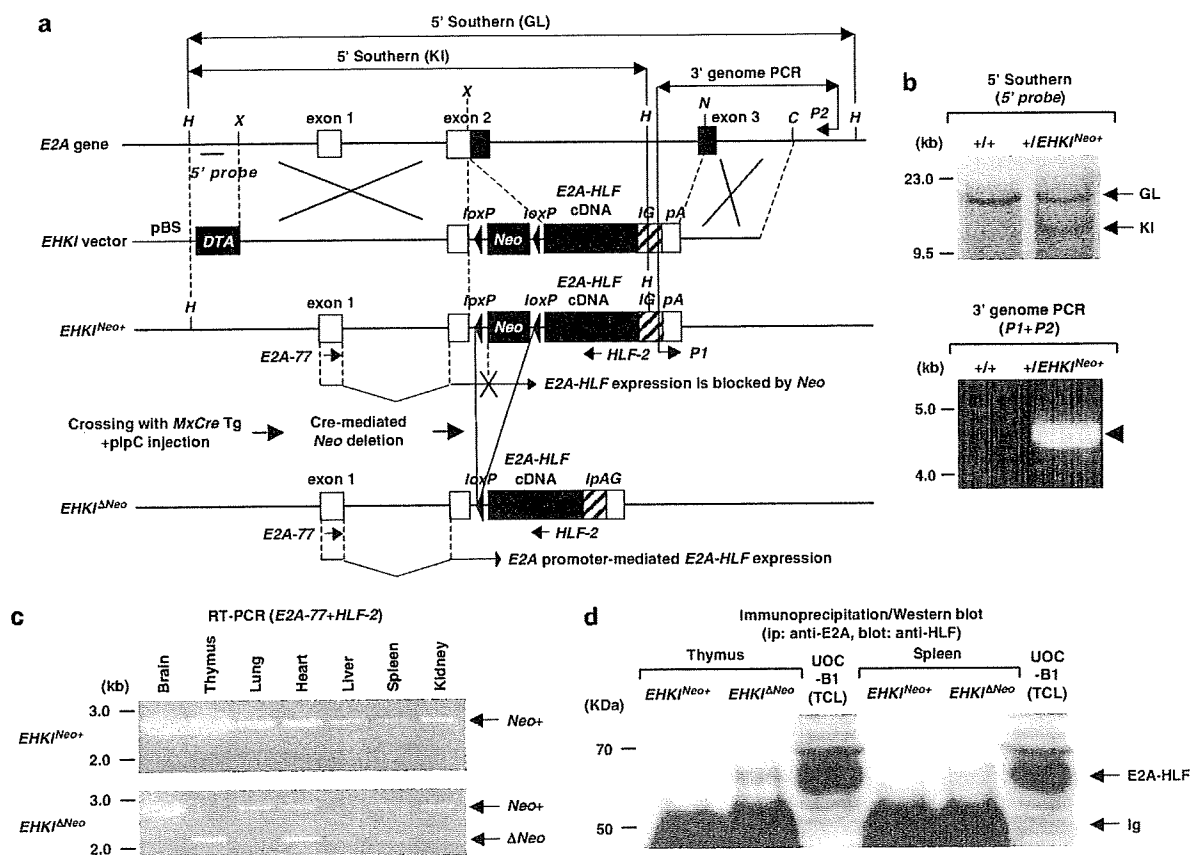
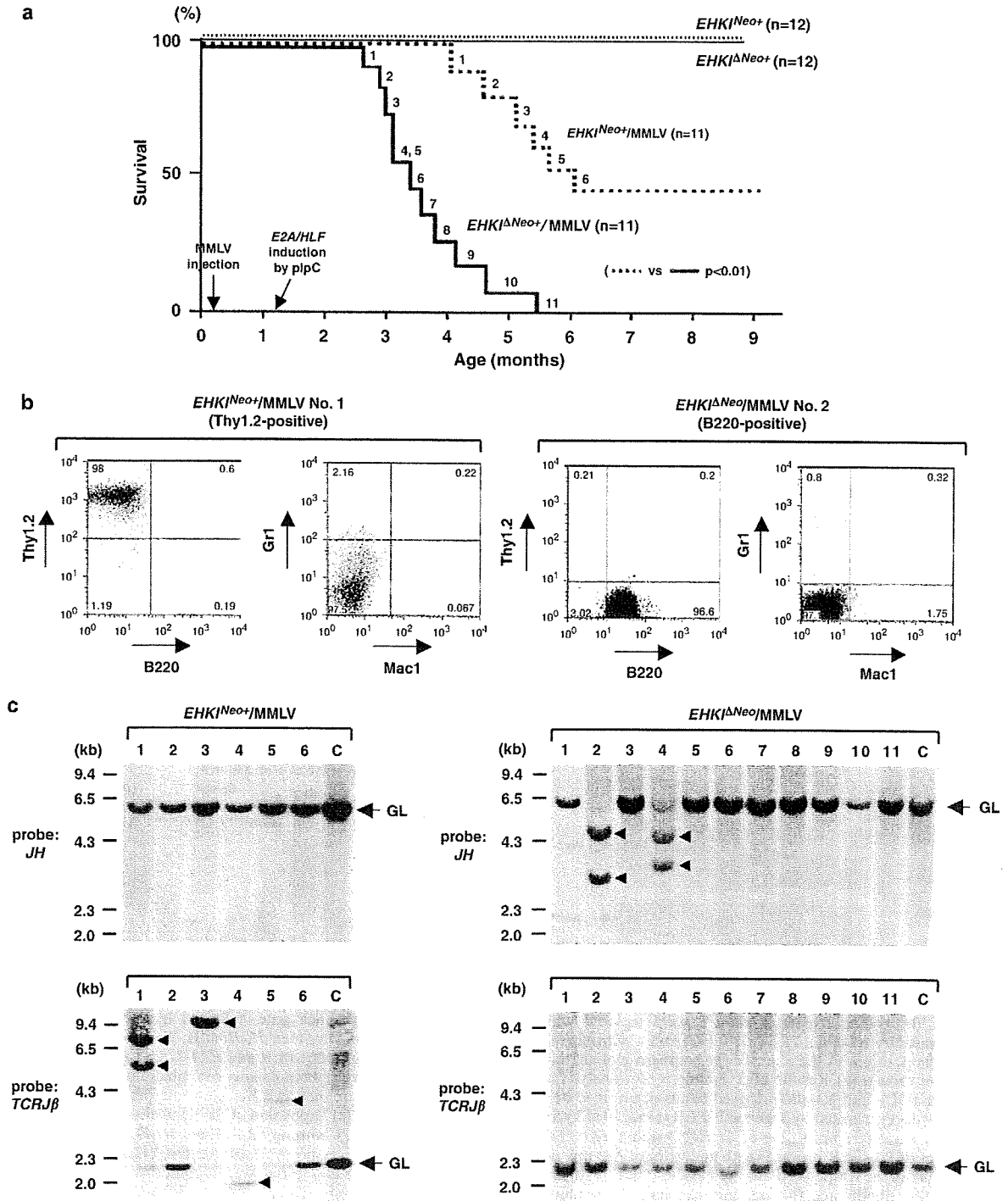


Figure 1 Generation of inducible knock-in (iKI) mice for *E2A-HLF* and the acquired expression of *E2A-HLF* in the hematopoietic tissues. (a) Schematic illustration of the iKI strategy. Part of the non-coding region of exon 2, the coding region of exon 2, intron 2 and part of the coding region of exon 3 were replaced with the *floxed neomycin* resistance gene, followed by *E2A-HLF* fusion complementary (cDNA), *IRES-GFP* (*IG*) and a *polyadenylation* signal (*pA*). Restriction enzymes: *H*, *HindIII*; *X*, *XbaI*; *N*, *NaeI*; *C*, *ClaI*. The positions of the 5' probe for Southern blot analysis, *P1* and *P2* primers for genomic PCR and *E2A-77* and *HLF-2* for RT-PCR are shown. (b) Results of 5' Southern blot analysis and 3' genomic PCR to detect homologous recombination. Positions of germline (GL)- and KI-allele-derived bands determined by 5' Southern blot analysis are indicated by arrows (upper panel) and the PCR product generated by 3' genomic PCR is indicated by an arrowhead (lower panel). (c) Expression of the KI allele-derived mRNA. mRNAs extracted from tissues of *EHKI^{Neo+}* and *EHKI^{ΔNeo}* mice were subjected to RT-PCR using *E2A-77* and *HLF-2* primers (see a). Positions of RT-PCR products with and without *Neo* are indicated by *Neo+* and Δ *Neo*, respectively. (d) Acquired *E2A-HLF* protein expression in the lymphoid tissues of *EHKI^{ΔNeo}* mice. Proteins extracted from the thymus and spleen were immunoprecipitated with an anti-*E2A* antibody, and the immunoprecipitants were blotted with an anti-*HLF* antibody. The positions of *E2A-HLF* protein and immunoglobulin (*Ig*) are indicated by arrows. Total cell lysate (TCL) from a *t(17;19)⁺* cell line, UOCB1, was used as a positive control.

samples that showed splenomegaly and lymph node swelling. In contrast, *EHK1^{ΔNeo}/MMLV* leukemic mice did not show thymic enlargement but showed splenomegaly, frequently associated with lymph node swelling. To determine the lineage of the leukemic cells, disaggregated cells were subjected to flow cytometric analysis. In *EHK1^{Neo+}/MMLV* mice, samples with

thymic enlargement (nos. 1 and 3–5) were positive for T-cell (Thy1.2) antigen, but negative for B-cell (B220), myeloid (Gr1) and macrophage (Mac1) antigens, whereas the other two samples lacking thymic enlargement (nos. 2 and 6) did not express any of Thy1.2, B220, Gr1 or Mac1 antigen. In *EHK1^{ΔNeo}/MMLV* mice, two samples (nos. 2 and 4) were positive



for B220 but negative for other antigens, whereas the remaining 9 samples (nos. 1, 3 and 5–11) did not express any of Thy1.2, B220, Gr1 or Mac1 antigen. Representative results of flow cytometric analysis of Thy1.2-positive $EHKI^{Neo+}$ /MMLV leukemic samples and B220-positive $EHKI^{\Delta Neo}$ /MMLV leukemic samples are shown in Figure 2b. As B-lineage leukemia is rarely developed in MMLV-infected mice, B-cell commitment of the two B220-positive samples (nos. 2 and 4 of $EHKI^{\Delta Neo}$ /MMLV mice) was further analyzed by using antibodies against CD19, BP1, CD20, CD43 and immunoglobulin M. The result showed that both samples were positive for CD19, BP1, CD20 and CD43 but negative for immunoglobulin M, showing that they were B-progenitor leukemias (Supplementary Figure 1).

The leukemic samples were then subjected to gene rearrangement analysis using *JH* and *TCRJ-β* probes. As expected from the results of flow cytometric analyses, Thy1.2-positive samples (nos. 1 and 3–5 of $EHKI^{Neo+}$ /MMLV group) showed rearranged bands in the *TCRJ-β* locus (indicated by arrowheads in the left lower panel of Figure 2c), and B220-positive samples (No. 2 and 4 of $EHKI^{\Delta Neo}$ /MMLV group) showed rearranged bands in the *IgH* locus (indicated by arrowheads in the right upper panel of Figure 2c), whereas other samples lacking lineage markers (nos. 2 and 6 of $EHKI^{Neo+}$ /MMLV mice and nos. 1, 3, and 5–11 of $EHKI^{\Delta Neo}$ /MMLV mice) showed germline patterns in both *IgH* and *TCRJ-β* regions. These results indicated that four $EHKI^{Neo+}$ /MMLV leukemias (nos. 1 and 3~5) were T-cell ALL and two $EHKI^{\Delta Neo}$ /MMLV leukemias (nos. 2 and 4) were B-lineage ALL, but others were lineage marker-negative leukemias that were derived from immature cells not yet committed to a specific cell lineage. The characteristics of $EHKI^{Neo+}$ /MMLV and $EHKI^{\Delta Neo}$ /MMLV leukemic mice are summarized in Table 1.

Identification of *Gfi1*, *Ikaros* and *Zfp521* as common integration sites (CISs) in leukemias developed in $EHKI^{\Delta Neo}$ /MMLV mice

To identify gene(s) whose altered expression cooperated with *E2A-HLF*, genomic DNAs extracted from leukemic samples of $EHKI^{\Delta Neo}$ /MMLV mice were subjected to inverse PCR (iPCR). DNAs from leukemias of $EHKI^{Neo+}$ /MMLV mice were also analyzed as controls. Genes identified by iPCR in $EHKI^{\Delta Neo}$ /MMLV and $EHKI^{Neo+}$ /

MMLV leukemic mice are listed in Supplementary Tables 1 and 2, respectively. In the iPCR products of $EHKI^{\Delta Neo}$ /MMLV mice, we found three CISs (shown by asterisks and bold type in Supplementary Table 1), all of which encode zinc-finger transcription factors.

First, in four leukemic samples (nos. 1, 6, 8 and 11), viruses were integrated in an ~10-kb upstream region (nos. 1, 8 and 11) or in the 3' untranslated region (no. 6) of *growth factor independent 1* (*Gfi1*) gene (upper panel of Figure 3a). Southern blot analysis using genomic fragments adjacent to the integration sites showed rearrangement bands in all the tumors (indicated by arrowheads in the lower left panel of Figure 3a), indicating that cells with these integration sites were predominant in the related tumors. In addition, northern blot analysis revealed that *Gfi1* mRNA expression levels were significantly enhanced in nos. 1, 8 and 11, and moderately increased in no. 6 when compared with those in a control spleen (C) and *Gfi1*-non-integrated samples (nos. 7 and 10, see Table 1 and Supplementary Table 1) (indicated by an arrow in the lower right panel of Figure 3a).

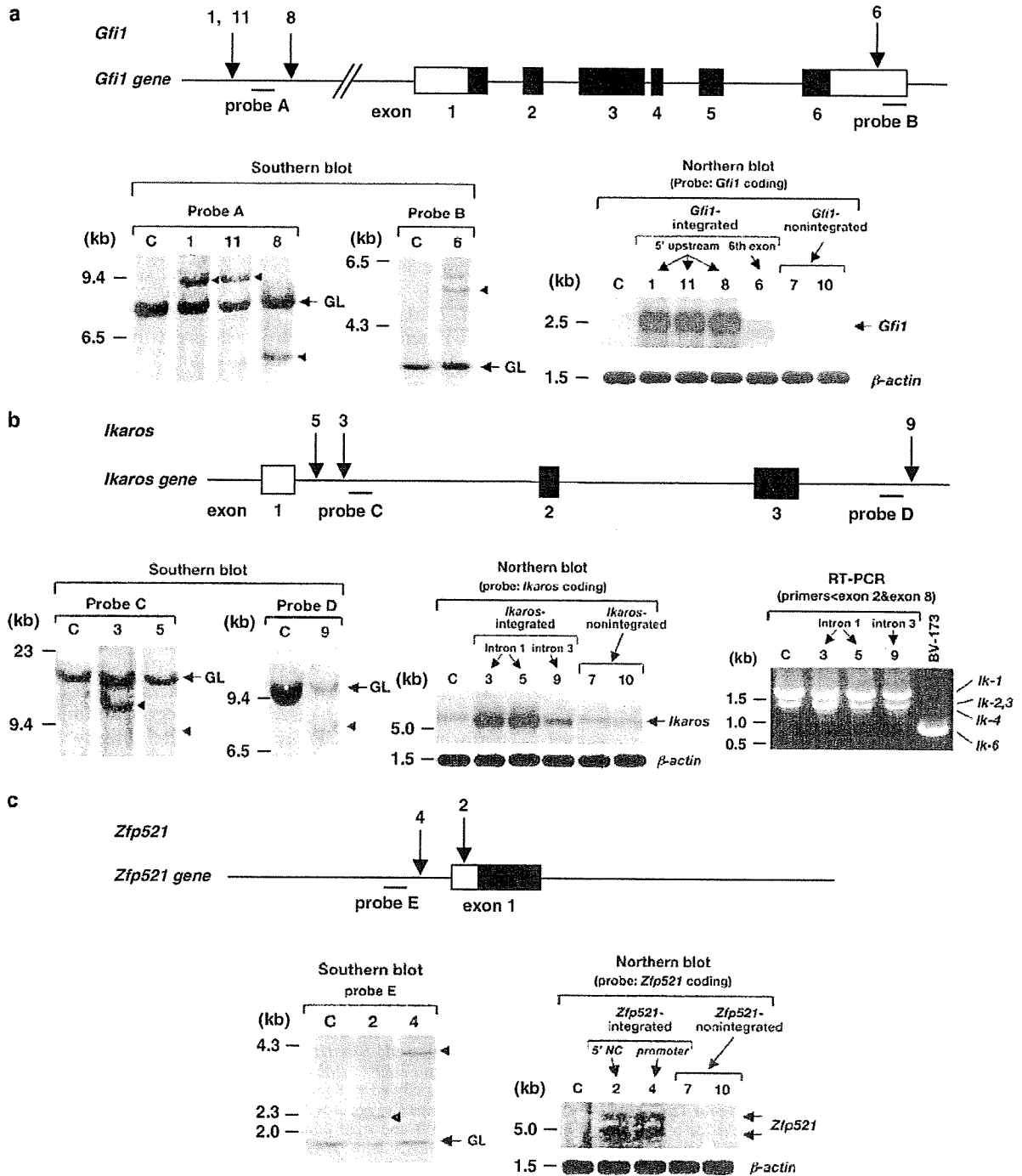
Second, *zinc-finger protein subfamily 1A1 isoform a* (*Zfp1a1*, also known as *Ikaros*, hereafter referred to as *Ikaros*) gene was the retroviral target in three samples (nos. 3, 5 and 9). Integrations occurred in intron 1 (nos. 3 and 5) and intron 3 (no. 9) (upper panel of Figure 3b). All these three samples (nos. 3, 5 and 9) carried rearranged bands (indicated by arrowheads in the lower left panel of Figure 3b) and showed enhanced *Ikaros* mRNA expression when compared with a control spleen (C) and *Ikaros*-non-integrated samples (nos. 7 and 10) (indicated by an arrow in the lower middle panel of Figure 3b). Previous reports showed that *Ikaros* contributes to leukemogenesis by an isoform change from normally expressed forms (*Ikaros* (Ik)-1, Ik-2, Ik-3 and Ik-4) to a shorter splicing variant, Ik-6, which suppresses downstream gene expressions in a dominant-negative manner (Nakayama *et al.*, 1999; Beverly and Capobianco, 2003). To analyze whether *Ik-6* mRNA was expressed in the three *Ikaros*-integrated samples, we performed RT-PCR to detect alternatively spliced mRNA isoforms. All three samples expressed *Ik-1*, -2, -3 and -4 mRNAs but did not express *Ik-6* mRNA (lower right panel of Figure 3b), indicating that the viral integrations simply upregulated *Ikaros* gene expression without affecting splicing.

Figure 2 Survival curves of $EHKI^{Neo+}$ and $EHKI^{\Delta Neo}$ mice with or without MMLV infection, and flow cytometric and gene rearrangement analyses of leukemic tissues of $EHKI^{Neo+}$ and $EHKI^{\Delta Neo}$ mice infected with MMLV ($EHKI^{Neo+}$ /MMLV and $EHKI^{\Delta Neo}$ /MMLV). (a) Survival curves of $EHKI^{Neo+}$, $EHKI^{\Delta Neo}$, $EHKI^{Neo+}$ /MMLV and $EHKI^{\Delta Neo}$ /MMLV mice. No disease was observed in $EHKI^{Neo+}$ or $EHKI^{\Delta Neo}$ mice (indicated by thin dotted and thin continuous lines, respectively). MMLV infection induced acute leukemias in both $EHKI^{Neo+}$ /MMLV and $EHKI^{\Delta Neo}$ /MMLV mice (indicated by thick dotted and thick continuous lines, respectively) and the $EHKI^{\Delta Neo}$ /MMLV mice showed higher morbidity and mortality than $EHKI^{Neo+}$ /MMLV mice. The diseased $EHKI^{Neo+}$ /MMLV and $EHKI^{\Delta Neo}$ /MMLV mice are numbered and the time points of MMLV injection and *E2A-HLF* induction by pIpC are indicated by arrows. (b) Representative results of a flow cytometric analysis. Leukemic cells in $EHKI^{Neo+}$ /MMLV and $EHKI^{\Delta Neo}$ /MMLV mice were stained with anti-Thy1.2, anti-B220, anti-Gr1 and anti-Mac1 antibodies and analyzed using a FACSCalibur. No. 1 of $EHKI^{Neo+}$ /MMLV leukemic mice that was positive for Thy1.2 but negative for other antigens and no. 2 of $EHKI^{\Delta Neo}$ /MMLV leukemic mice that was positive for B220 but was negative for other antigens are shown in the left and right panels, respectively. (c) Results of gene rearrangement analysis. DNAs extracted from leukemic tissues of $EHKI^{Neo+}$ /MMLV and $EHKI^{\Delta Neo}$ /MMLV mice were digested with *EcoRI* and blotted with *JH* (upper panels) and *TCRJ-β* (lower panels) probes. Germline (GL) and rearranged bands are indicated by arrows and arrowheads, respectively.

Finally, *zinc-finger protein 521* (*Zfp521*, also known as *Evi3*) gene was integrated by retroviruses in two B-lineage leukemia mice (nos. 2 and 4). One integration site was in the 5' upstream region and the other was in the 5' untranslated region of exon 1 (upper panel of Figure 3c). Both samples showed rearranged gene patterns (indicated by arrowheads in the lower left panel of Figure 3c) and showed enhanced *Zfp521* mRNA expression when compared with a control spleen

(C) and *Zfp521*-non-integrated samples (nos. 7 and 10) (indicated by arrows in the lower right panel of Figure 3c).

On the other hand, among the iPCR products of *EHKI^{Neo+}/MMLV* leukemic mice, we detected one CIS, which was *Abelson helper integration site 1* (*Ahi1*) gene (shown by asterisks and bold type in Supplementary Table 2). This CIS was found in samples 3 and 4, in which retroviruses were integrated in introns 9 and 23,



respectively (upper panel of Supplementary Figure 2). Southern blot analyses using genomic fragments adjacent to the integration sites detected rearranged bands, indicating that these are the major integration sites in the related tumors (indicated by arrowheads in the lower panel of Supplementary Figure 2).

Taken together, the iPCR analysis revealed that the virus integrations in three transcription factors, *Gfi1*, *Ikaros* and *Zfp521*, were preferentially associated with *EHK1^{ΔNeo}/MMLV* leukemias and strongly suggested that overexpression and/or aberrant expression of these gene products would have a cooperative role with *E2A-HLF* in the leukemogenic process.

Enhanced expression of ZNF521 in human leukemic cell lines with t(17;19)

To analyze the clinical significance of the three transcription factors identified in *EHK1^{ΔNeo}/MMLV* leukemias (*Gfi1*, *Ikaros* and *Zfp521*) in human leukemia with t(17;19), we examined mRNA expression levels of the three genes in t(17;19)-positive (t(17;19)⁺) ALL lines and in control B-lineage ALL lines without t(17;19). Cell lines were used instead of primary patient samples, because t(17;19)⁺ ALL constitutes only a small subset of B-precursor leukemias (Look, 1997).

The results obtained using quantitative RT-PCR are shown in Figure 4. *Gfi1* mRNA levels were mostly constant in control and t(17;19)⁺ cell lines, but the overall *Gfi1* expression in t(17;19)⁺ lines was lower than that in control lines (Figure 4, left panel). As for *Ikaros*, mRNA expression levels were relatively stable in control lines but were varied among t(17;19)⁺

lines, and the mean *Ikaros* expression in t(17;19)⁺ lines was slightly lower than that in control lines (Figure 4, middle panel). These results indicated that the expression levels of *Gfi1* and *Ikaros* were not enhanced in t(17;19)⁺ cell lines.

In contrast, the expression levels of *ZNF521*, the human homolog of *Zfp521* (also known as *early hematopoietic zinc-finger protein (EHZF)*), were found to be consistently higher in t(17;19)⁺ lines than in control lines. Two lines showed approximately 10-fold upregulation and one line showed more than >50-fold upregulation (indicated by arrows and an arrowhead in the right panel of Figure 4). These results strongly suggest that the overexpression of *ZNF521* would be clinically relevant to t(17;19)-positive B-lineage ALL.

Expression of E2A-HLF and Zfp521 conferred a growth advantage on B-progenitor cells, and both knocked-in for E2A-HLF and transgenic for Zfp521 mice developed B-lineage ALL

We finally analyzed the *in vivo* cooperative role of *Zfp521* with *E2A-HLF*. For this purpose, we generated transgenic mice for *Zfp521* and crossed them with *EHK1^{ΔNeo}* mice. To express *Zfp521* in lymphoid cells, *Zfp521* complementary DNA with an *HA* tag (*Zfp521HA*) was subcloned into *EμSV* vector, which has been successfully used to express target genes in the lymphoid lineage (Rosenbaum et al., 1990) (Figure 5a). Among several transgenic lines established (*EμSV/Zfp521*), mice of a line that expresses *Zfp521HA* at a high level in lymphoid cells (data not shown) were chosen and crossed with *EHK1^{ΔNeo}* mice.

Figure 3 Retroviral integration sites, gene rearrangements and altered expression patterns in CISs detected in *EHK1^{ΔNeo}/MMLV* leukemic mice (a) *Gfi1* gene. Upper panel: schematic illustrations of viral integration sites in the *Gfi1* gene. Exons are boxed, and the coding and non-coding regions are indicated by black and white boxes, respectively. Viral integration sites are indicated by vertical arrows with the related mouse identification numbers (nos. 1, 11, 6 and 8). Positions of probes used for Southern blot analyses are also shown. Lower left panel: Southern blot analysis for gene rearrangements. DNAs extracted from a control spleen (C) and *Gfi1*-integrated *EHK1^{ΔNeo}/MMLV* mice (nos. 1, 11, 6 and 8) were digested with *Bam*HI and probed with the adjacent genomic fragment shown in (a) (probe A for nos. 1, 11 and 6, and probe B for no. 8). Germline (GL) and rearranged bands are indicated by arrows and arrowheads, respectively. Lower right panel: Northern blot analysis for *Gfi1* mRNA expression. mRNAs of a control spleen (C) and *Gfi1*-integrated *EHK1^{ΔNeo}/MMLV* mice (nos. 1, 11, 6 and 8) were probed with the *Gfi1* coding region. *Gfi1*-non-integrated tumors (nos. 7 and 10) were also used as controls. The position of *Gfi1* mRNA is indicated by an arrow and *β-actin* hybridization served as the internal control. (b) *Ikaros* gene. Upper panel: schematic illustrations of virus integration sites in the *Ikaros* gene. Exons are boxed, and the coding and noncoding regions are indicated by black and white boxes, respectively. Viral integration sites are indicated by vertical arrows with the related mouse identification numbers (no. 3, 5 and 9). Positions of probes used for Southern blot analyses are also shown. Lower left panel: Southern blot analysis for gene rearrangements. DNAs extracted from a control spleen (C) and *Ikaros*-integrated *EHK1^{ΔNeo}/MMLV* mice (nos. 3, 5 and 9) were digested with *Bam*HI and probed with the adjacent genomic fragment shown in (a) (probe C for nos. 3 and 5, probe D for no. 9). Germline (GL) and rearranged bands are indicated by arrows and arrowheads, respectively. Lower middle panel: Northern blot analysis for *Ikaros* mRNA expression. mRNAs of a control spleen (C) and *Ikaros*-integrated *EHK1^{ΔNeo}/MMLV* mice (nos. 3, 5 and 9) were probed with the *Ikaros* coding region. *Ikaros*-non-integrated tumors (nos. 7 and 10) were also used as controls. The position of *Ikaros* mRNA is indicated by an arrow and *β-actin* hybridization served as the internal control. Lower right panel: RT-PCR for *Ikaros* mRNA isoforms. mRNAs of a control spleen (C) and *Ikaros*-integrated *EHK1^{ΔNeo}/MMLV* mice (nos. 3, 5 and 9) were subjected to RT-PCR to detect *Ikaros* mRNA isoforms. The positions of isoforms *Ik1*, *Ik2*, *Ik3*, *Ik4* and *Ik6* are indicated. A human CML BC cell line, BV173, was used to show the position of *Ik-6* (Nakayama et al., 1999). (c) *Zfp521* gene. Upper panel: Schematic illustrations of viral integration sites in the *Zfp521* gene. Exons are boxed, and the coding and noncoding regions are indicated by black and white boxes, respectively. Virus integration sites are indicated by vertical arrows with the related mouse identification numbers (nos. 2 and 4). Position of a probe used for Southern blot analyses is also shown. Lower left panel: Southern blot analysis of gene rearrangements. DNAs extracted from a control spleen (C) and *Zfp521*-integrated *EHK1^{ΔNeo}/MMLV* mice (nos. 2 and 4) were digested with *Bam*HI and probed with the adjacent genomic fragment shown in (a) (probe E). Germline (GL) and rearranged bands are indicated by an arrow and arrowheads, respectively. Lower right panel: Northern blot analysis for *Zfp521* mRNA expression. mRNAs of a control spleen (C) and *Zfp521*-integrated *EHK1^{ΔNeo}/MMLV* mice (nos. 2 and 4) were probed with the *Zfp521* coding region. *Zfp521*-non-integrated tumors (nos. 7 and 10) were also used as controls. Two alternatively spliced forms of *Zfp521* mRNA are indicated by arrows and *β-actin* hybridization served as the internal control.

Table 1 Characteristics of *EHKI^{Neo+}/MMLV* and *EHKI^{ΔNeo}/MMLV* leukemic samples

Mouse no.	Age at disease (month)	PB parameters			Macroscopic tumor sites	Surface markers				Gene status		Diagnosis	Major integration site
		WBC ($\times 10^3/\mu\text{l}$)	Hb (g dL^{-1})	Plt ($\times 10^3/\mu\text{l}$)		Thy1.2	B220	Grl	Mac1	JH	TCRJ- β		
<i>EHKI^{Neo+}/MMLV</i>													
1	4.0	86.5	5.6	50.3	Thy, Spl	(+)	(-)	(-)	(-)	G/G	G/R	T-cell ALL	ND
2	4.5	25.1	16.7	26.3	Spl, LN	(-)	(-)	(-)	(-)	G/G	G/G	Lin ⁻ AL	ND
3	5.0	33.2	13.1	14.8	Thy, Spl	(+)	(-)	(-)	(-)	G/G	G/R	T-cell ALL	<i>Ahil</i> (23rd intron)
4	5.3	15.1	13.5	28.5	Thy, Spl	(+)	(-)	(-)	(-)	G/G	G/R	T-cell ALL	<i>Ahil</i> (9th intron)
5	5.5	67.5	7.1	44.9	Thy, Spl, LN	(+)	(-)	(-)	(-)	G/G	G/R	T-cell ALL	ND
6	6.0	15.3	12.5	38.8	Spl, LN	(-)	(-)	(-)	(-)	G/G	G/G	Lin ⁻ AL	ND
<i>EHKI^{ΔNeo}/MMLV</i>													
1	2.6	16.3	10.0	30.3	Spl, LN	(-)	(-)	(-)	(-)	G/G	G/G	Lin ⁻ AL	<i>Gfi1</i> (5' upstream)
2	3.1	16.0	14.0	46.1	Spl, LN	(-)	(+)	(-)	(-)	R/R	G/G	B-cell ALL	<i>Zfp521</i> (5' noncoding)
3	3.2	1.0	4.7	7.1	Spl	(-)	(-)	(-)	(-)	G/G	G/G	Lin ⁻ AL	<i>Ikaros</i> (1st intron)
4	3.3	15.1	13.2	20.5	Spl, LN	(-)	(+)	(-)	(-)	R/R	G/G	B-cell ALL	<i>Zfp521</i> (5' upstream)
5	3.3	21.3	12.2	41.2	Spl	(-)	(-)	(-)	(-)	G/G	G/G	Lin ⁻ AL	<i>Ikaros</i> (1st intron)
6	3.4	15.7	13.3	19.4	Spl	(-)	(-)	(-)	(-)	G/G	G/G	Lin ⁻ AL	<i>Gfi1</i> (3' noncoding)
7	3.6	36.0	12.5	21.8	Spl, LN	(-)	(-)	(-)	(-)	G/G	G/G	Lin ⁻ AL	ND
8	3.8	54.9	11.5	16.7	Spl	(-)	(-)	(-)	(-)	G/G	G/G	Lin ⁻ AL	<i>Gfi1</i> (5' upstream)
9	4.0	96.8	6.0	18.9	Spl, LN	(-)	(-)	(-)	(-)	G/G	G/G	Lin ⁻ AL	<i>Ikaros</i> (3rd intron)
10	4.5	20.5	5.3	20.2	Spl	(-)	(-)	(-)	(-)	G/G	G/G	Lin ⁻ AL	ND
11	5.6	2.1	2.7	51.9	Spl, LN	(-)	(-)	(-)	(-)	G/G	G/G	Lin ⁻ AL	<i>Gfi1</i> (5' upstream)

Abbreviations: *Ahil*, *Abelson helper integration site 1*; ALL, acute lymphoblastic leukemia; G, germline; *Gfi1*, *growth factor independent 1*; Hb, hemoglobin; *Ikaros*, *zinc-finger protein subfamily 1A1 isoform a (Zfp1a1)*, also known as *Ikaros*; Lin⁻, lineage marker-negative; LN, lympho node; Mac1, macrophage antigen-1; MMLV, Moloney murine leukemia virus; ND, not determined; PB, peripheral blood; plt, platelet; R, rearranged; Spl, spleen; Thy, thymus; WBC, white blood cell; *Zfp521*, *zinc-finger protein 521*.

The survival curves of the offspring are shown in Figure 5b. During about 6 months of observation period, half of the compound mice developed acute leukemia (thick continuous line), whereas none of *EHKI^{ΔNeo}* or *E μ SV/Zfp521* alone showed hematological disease (thin continuous and thin dotted lines). All the leukemic cells were positive for B220 but negative for Thy1.2, Mac1 or Grl (data not shown) and showed rearrangement patterns in the *IgH* region (Figure 5c). The expression of *E2A-HLF* and *Zfp521HA* in the tumor tissues was confirmed by RT-PCR using primer sets specific for transcripts from *E2A-HLF* knocked-in allele (*E2A-77 + HLF-2*, see Figure 1c) and *E μ SV/Zfp521* transgene (*SV40-1 + SV40-2*, see Figure 5a), respectively (Figure 5d).

As *EHKI^{ΔNeo}* mice with *Zfp521* overexpression exclusively developed B-lineage leukemia (nos. 1–5 of *EHKI^{ΔNeo} × E μ SV/Zfp521HA* mice and nos. 2 and 4 of *EHKI^{ΔNeo}/MMLV* mice), we analyzed the proliferative potential of B-progenitor cells in *EHKI^{ΔNeo}* mice and *E μ SV/Zfp521* mice. For this purpose, BM cells extracted from both types of mice and their controls were subjected to flow cytometric analysis and B-cell colony formation assay. As shown in Figure 5e, both of *EHKI^{ΔNeo}* knock-in and *E μ SV/Zfp521* transgenic BM cells contained increased number of B-cell precursors and possessed an enhanced B-cell colony formation ability when compared with those of control *EHKI^{Neo+}* and *wild-type* mice (as for the results of flow cytometry, see also Supplementary Figure 3). These results indicated that expression of *E2A-HLF* and *Zfp521* rendered a proliferative ability to B-progenitor cells and suggest that their coexpression synergizes and contributes to the development of B-lineage leukemia.

Discussion

In earlier studies, we analyzed the role of *E2A-HLF* by a transgenic approach and showed that the expression of *E2A-HLF* under the control of lymphocyte-specific promoters perturbs normal lymphocyte development and contributes to the development of ALL (Honda et al., 1999). However, in contrast with the fact that human leukemia harboring t(17;19) exclusively shows a B-cell phenotype, all the *E2A-HLF* transgenic mice developed T-cell ALL (Honda et al., 1999). In this work, to circumvent this problem and to create a mouse model that further mimics human t(17;19)-positive ALL, we generated mice in which *E2A-HLF* was inducibly expressed under the control of the native *E2A* promoter.

Stimulation of *EHKI^{Neo+}/MxCre* mice with pIpC produced *EHKI^{ΔNeo}* mice, in which the deletion of the *floxed Neo* gene induced the expression of the *E2A-HLF* chimeric gene product in the hematopoietic tissues (Figures 1c and d). However, no disease was developed in *EHKI^{ΔNeo}* mice during the long-term observation period (Figure 2a, thin lines), indicating that the acquired expression of *E2A-HLF per se* is insufficient for the development of leukemia. This finding is in line with previous reports showing that iKI mice of other leukemogenic transcription factor chimeras, such as *AML1-ETO* and *MLL-CBP*, did not show hematopoietic disorders, and secondary mutations induced by *N*-methyl-*N*-nitrosourea or irradiation were required to induce a fully malignant phenotype (Higuchi et al., 2002; Wang et al., 2005). In this study, to introduce additional gene alterations, we used RIM, as it not only

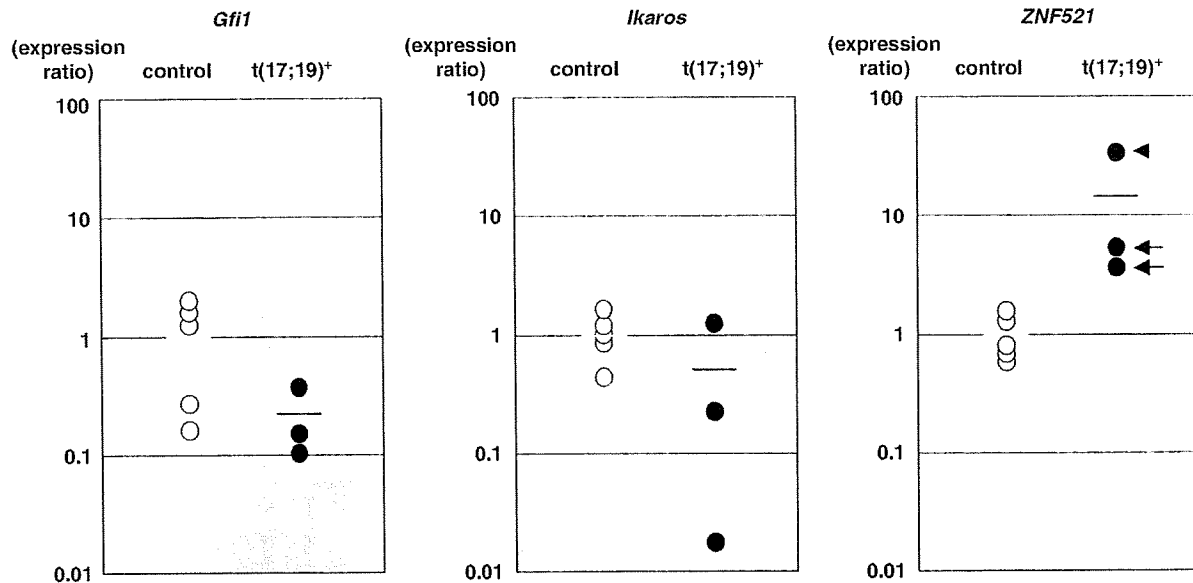


Figure 4 Quantitative mRNA expression of *Gfi1*, *Ikaros* and *ZNF521* in human leukemic cell lines with or without t(17;19). The mRNA expression levels in five control B-progenitor cell lines (control) and three t(17;19)-positive cell lines (t(17;19)⁺) relative to the mean of the control cell lines (white bar) are indicated by white and black circles, respectively. The mean of t(17;19)⁺ cell lines is indicated by a black bar. The relative expression ratio (vertical bar) is shown on a logarithmic scale. The high expression patterns of *ZNF521* in t(17;19)⁺ cell lines are indicated by arrows and an arrowhead (right panel).

successfully induces mutations in the mouse genome but also has the advantage that the mutated genes can be detected by iPCR using the tumor genome and virus-specific primers (Jonkers and Berns, 1996; Mikkers and Berns, 2003; Nakamura, 2005).

MMLV infection induced acute leukemias in *EHKI^{ΔNeo}* mice at a higher frequency and with a shorter latency than in control *EHKI^{Neo±}* mice (Figure 2a, thick lines). This finding indicates that *E2A-HLF* possesses an oncogenic potential in hematopoietic cells, which was accelerated by viral integrations. In addition, it is to be noted that the phenotypes of the leukemias were different between *EHKI^{ΔNeo}/MMLV* and *EHKI^{Neo±}/MMLV* mice. In contrast with the fact that *EHKI^{Neo±}/MMLV* mice mainly developed T-cell ALL (four of six samples), *EHKI^{ΔNeo}/MMLV* mice showed B-progenitor ALL (two samples) and lineage marker-negative leukemias (other nine samples; Figures 2b and c and Table 1).

Previous studies showed that MMLV induces T-cell leukemia in wild-type mice very efficiently, at almost 100% penetrance (Jonkers and Berns, 1996; Mikkers and Berns, 2003). Thus, the reason why all the *EHKI^{Neo±}/MMLV* mice did not develop T-cell ALL is unclear. One possibility is the low copy number of the virus. This idea is supported by our previous RIM study, in which only ~60% of the MMLV-infected wild-type mice developed T-cell ALL (Mizuno et al., 2008). In addition, it also remains to be clarified why leukemias of *EHKI^{ΔNeo}/MMLV* mice showed B-progenitor and lineage marker-negative phenotypes. A previous report showed that transgenic background affected the disease phenotype of MMLV-induced leukemia. MMLV-infected wild-type mice exclusively developed

T-ALL, whereas virus-infected *Em/bcl2* transgenic mice mainly succumbed to B-lineage leukemia (Shinto et al., 1995). Therefore, it could be postulated that induced expression of *E2A-HLF* might exert its oncogenic potential in hematopoietic cells differentiating from a very early to the B-cell committed stage. This idea is in line with the finding that B-cell precursors in the *EHKI^{ΔNeo}* BM possessed a proliferative ability (Figure 5e) and is also in good agreement with the result that t(17;19)-positive human leukemia is exclusively of early B-progenitor phenotype (Inaba et al., 1992).

Intriguingly, pathological analysis revealed that microthrombi, a clinical feature of coagulopathy, were observed in the lung of three *EHKI^{ΔNeo}/MMLV* leukemic mice with relatively low platelet count (nos. 3, 6 and 8, indicated by arrows in Supplementary Figure 4, and see also Table 1). Microthrombus formation was not observed in control *EHKI^{Neo±}/MMLV* leukemic tissues and has not been detected in our previous RIM studies (Mizuno et al., 2008; Miyazaki et al., 2009), strongly suggesting that this pathological abnormality is specific for *E2A-HLF*-expressing leukemic mice. Taken together, our mouse model would not only reflect the oncogenicity of *E2A-HLF* in hematopoietic progenitor cells differentiating to the B-cell lineage (Inaba et al., 1992), but also represent the coagulopathic property of t(17;19)-positive leukemic cells (Hunger, 1996).

iPCR of *EHKI^{ΔNeo}/MMLV* leukemic mice identified *Gfi1*, *Ikaros* and *Zfp521* as CISs, whereas that of *EHKI^{Neo±}/MMLV* leukemic mice detected *Ahil* as a CIS (Supplementary Tables 1 and 2). Major contribution of the CISs to tumor formation was confirmed

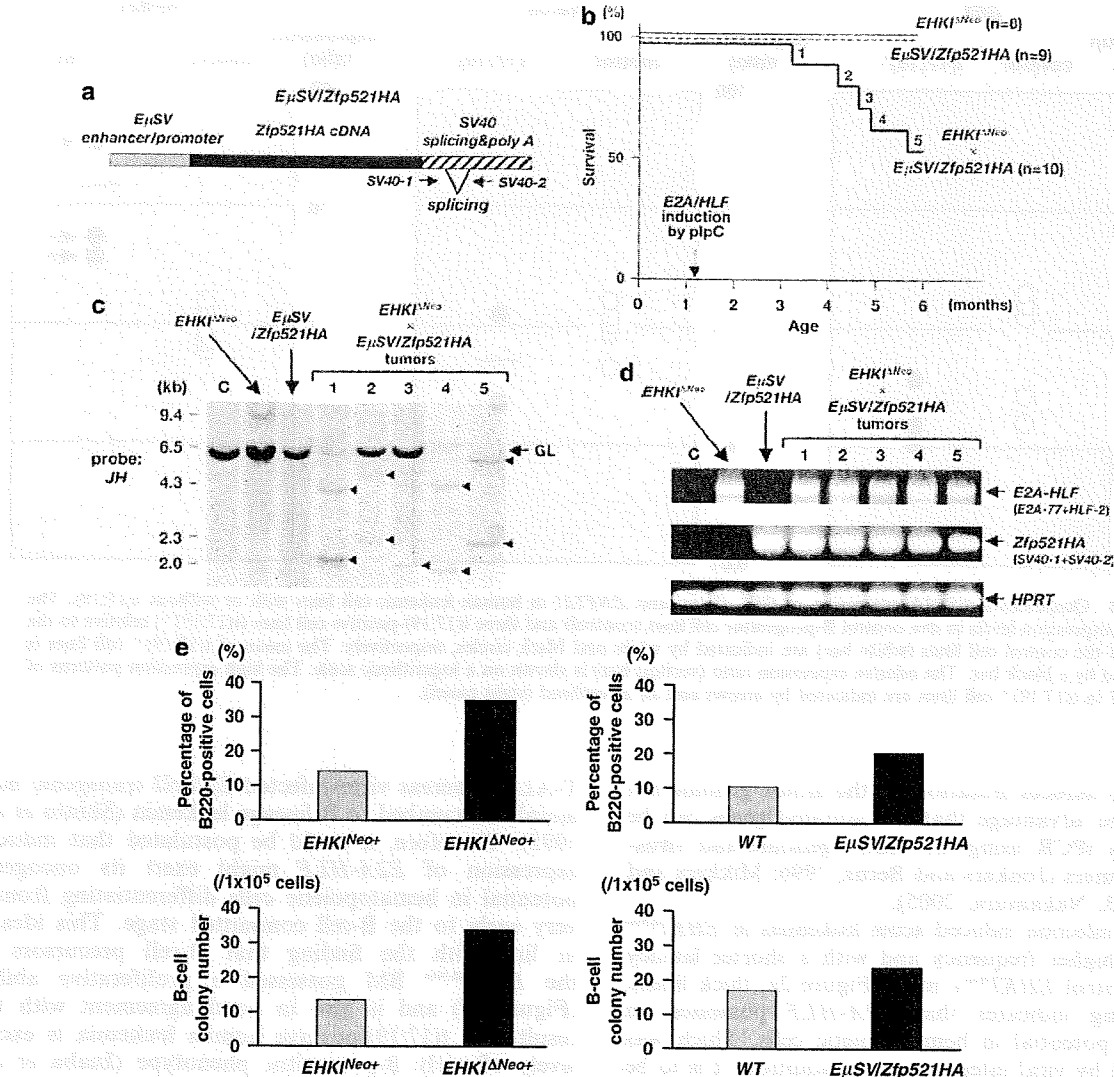


Figure 5 Cooperative oncogenicity of *Zfp521* with *E2A-HLF* and increased proliferative ability of B-cell precursors in *EHK1^{ΔNeo}* knock-in and *EμSV/Zfp521HA* transgenic mice. (a) Schematic structure of the transgene for generating *EμSV/Zfp521HA* transgenic mice. *EμSV* enhancer/promoter, *Zfp521HA* complementary (c)DNA, *SV40* splicing and *polyA* signals are shown as gray, black and shaded boxes, respectively. The positions of the splicing and primers encompassing the splicing signal (*SV40-1* and *SV40-2*) are indicated. (b) Survival curves of *EHK1^{ΔNeo}* mice, *EμSV/Zfp521HA* mice and *EHK1^{ΔNeo} × EμSV/Zfp521HA* mice. During the observation period of 6 months, whereas no disease was observed in *EHK1^{ΔNeo}* and *EμSV/Zfp521HA* mice (thin continuous and thin dotted lines), half of *EHK1^{ΔNeo} × EμSV/Zfp521HA* mice died of leukemia (thick continuous line). The time point of *E2A-HLF* induction by plpC is indicated by an arrow and the diseased *EHK1^{ΔNeo} × EμSV/Zfp521HA* mice are numbered. (c) Gene rearrangement analysis of leukemias developed in *EHK1^{ΔNeo} × EμSV/Zfp521HA* mice. DNAs extracted from a control spleen (C), an *EHK1^{ΔNeo}* mouse spleen, an *EμSV/Zfp521HA* mouse spleen and five tumors developed in *EHK1^{ΔNeo} × EμSV/Zfp521HA* mice were digested with *EcoRI* and blotted with the *JH* probe. Germline (GL) and rearranged bands are indicated by an arrow and arrowheads, respectively. (d) Expression of *E2A-HLF* and *Zfp521HA* in leukemias developed in *EHK1^{ΔNeo} × EμSV/Zfp521HA* mice. RNAs extracted from a control spleen (C), an *EHK1^{ΔNeo}* mouse spleen, an *EμSV/Zfp521HA* mouse spleen and five tumors developed in *EHK1^{ΔNeo} × EμSV/Zfp521HA* mice were subjected to RT-PCR for *E2A-HLF* (upper panel) and *Zfp521HA* (middle panel). All the tumors expressed both iKI allele- and transgenic allele-derived products. *HPRT* RT-PCR served as the internal control (lower panel). (e) Results of flow cytometric analysis (upper panels) and B-cell colony formation assay (lower panels). Upper panels: BM cells extracted from *EHK1^{Neo+}* and *EHK1^{ΔNeo}* mice (left panels) and *wild-type* (WT) and *EμSV/Zfp521HA* mice (right panels) were analyzed by flow cytometry using anti-B220 and anti-Thy1.2 antibodies. The mean percentages of B220-positive cells of three independent mice are shown. Lower panels: BM cells extracted from the same types of mice were subjected to B-cell colony formation assay. The mean colony numbers of three independent mice are shown.

using Southern blot analysis (Figure 3 and Supplementary Figure 2), and aberrant expression of the gene products in the related leukemic tissues in *EHK1^{ΔNeo}/MMLV* mice was shown using northern blot analysis

(Figure 3). These results indicated that the three transcription factors, *Gfi1*, *Ikaros* and *Zfp521*, would have a cooperative role preferentially in *E2A-HLF*-mediated leukemogenesis.

Gfi1 was originally cloned as a gene whose activation in T-cells by MMLV insertion leads to IL-2 independence (Gilks *et al.*, 1993) and was subsequently found as a target in tumors that developed in MMLV-infected transgenic mice (Zörnig *et al.*, 1996; Scheijen *et al.*, 1997). Transgenic studies showed that the aberrant *Gfi1* expression itself does not efficiently induce leukemia, but exerts its oncogenic potential when coexpressed with other genes such as *Myc* or *Pim*. Thus, our results suggested that *E2A-HLF* might be a new candidate gene that cooperates with *Gfi1*.

The frequent retroviral integration in the *Ikaros* gene (3 of 11 samples, see Figure 3b and Table 1) is to be noted, as in a world-wide RIM screen (<http://RTCGD.ncicrf.gov>), only four *Ikaros*-integrated samples were reported among more than several hundred CISs. A previous study using MMLV-infected *lck/Notch1C* (the active form of *Notch1*) transgenic mice identified *Ikaros* as a CIS (Beverly and Capobianco, 2003), in which MMLV was preferentially integrated in intron 2 and induced the expression of the dominant interfering *Ik-6*. However, in this study, the integration of MMLV in introns 1 or 3 increased expression of normal *Ikaros* isoforms (*Ik-1* to *Ik-4*) but did not induce *Ik-6* expression (Figure 3b). These results suggested that *Ikaros* might contribute to leukemogenesis through different mechanisms, depending on the partner genes.

Identification of *Zfp521* as a CIS is particularly interesting, as both *Zfp521*-integrated mice (nos. 2 and 4) developed B-progenitor ALL (Figure 2 and Table 1), which corresponds to the phenotype of human t(17;19)-positive leukemia. Therefore, it could be strongly postulated that *ZNF521*, the human counterpart of *Zfp521*, has an important role in the leukemogenic process of ALL with t(17;19). Indeed, among three zinc-finger proteins isolated as CISs in *EHK1^{ΔNeo}/MMLV* leukemic mice, we found that only *ZNF521* was consistently overexpressed in human ALL cell lines harboring t(17;19) (Figure 4). In addition, both knocked-in for *E2A-HLF* and transgenic for *Zfp521* mice frequently developed B-lineage ALL (Figure 5), which showed the *in vivo* cooperative oncogenicity of *Zfp521* with *E2A-HLF*.

Zfp521 was originally identified as a retroviral integration site in AKXD mice with B-lineage lymphomas, which encodes a transcription factor with multiple zinc-fingers (Warming *et al.*, 2003). Although the molecular mechanisms by which aberrant expression of *Zfp521* contributes to leukemogenesis are not fully understood, one possibility is that *Zfp521* impairs normal B-cell development by inhibiting the function of EBF1 (Hentges *et al.*, 2005), a transcription factor required for B-cell development (Lin and Grosschedl, 1995). Another possibility is that *Zfp521* itself functions as a *trans*-repressor and perturbs normal hematopoietic cell development through a N-terminal conserved domain that recruits and interacts with the nucleosome remodeling and deacetylase corepressor complex (Bond *et al.*, 2008).

Zfp521 was found to be widely associated with B-cell leukemia/lymphoma in mouse, whereas aberrant expression of *ZNF521* is rarely found in B-progenitor ALL in human (Bond *et al.*, 2008). Considering that t(17;19)-positive leukemia is found in a small portion of human

ALL (Look, 1997), it might be postulated that *Zfp521/ZNF521* is a preferential partner of *E2A-HLF* and the cooperative oncogenicity of these two genes constitutes a small subset of human B-lineage ALL.

In this report, we applied retrovirus insertional mutagenesis to *E2A-HLF* iKI mice, isolated *Gfi1*, *Ikaros* and *Zfp521* as cooperative genes with *E2A-HLF* and identified *Zfp521/ZNF521* to be a cooperative gene for *E2A-HLF* in t(17;19)-positive B-lineage leukemia. These results provide evidence that multi-step gene alterations are required for leukemogenesis and prove that the iKI system in conjunction with RIM is a valuable tool for identifying genes whose aberrant expression contributes to the malignant transformation of hematopoietic cells.

Materials and methods

Construction of iKI and transgenic vectors and generation of knock-in and transgenic mice

Detailed procedures for construction of iKI and transgenic vectors and for generation of iKI and transgenic mice are described in Supplementary Table 3.

Primer sequences

All the primer sequences used in this study are shown in Supplementary Table 4.

RT-PCR

To detect *E2A-HLF* mRNA, RT-PCR was performed using *E2A-77* and *HLF-2* primers that were derived from *E2A* exon 1 and the *HLF* portion of *E2A-HLF* complementary DNA as previously described (Miyazaki *et al.*, 2002). *Zfp521* mRNA expression was examined by RT-PCR using *SV40-1* and *SV40-2* primers that encompass the *SV40* splicing signal as described (Honda *et al.*, 1995). To detect *Ikaros* mRNA isoforms, RT-PCR was performed as described elsewhere (Nakayama *et al.*, 1999). To quantitate mRNA expression in human cell lines and mouse tissues, quantitative RT-PCR was performed using primers listed in Supplementary Table 4 as previously described (Miyazaki *et al.*, 2002).

Immunoprecipitation and western blot

Tissues were homogenized in 1% Triton lysis buffer and immunoprecipitation and western blot were performed as previously described (Honda *et al.*, 1999). Positive signals were visualized using enhanced chemiluminescence.

MMLV infection and identification of retroviral integration sites

Preparation and infection of retroviruses were performed as previously described (Wolff *et al.*, 2003a, b). Identification of retroviral integration sites was performed essentially as described elsewhere (Yamashita *et al.*, 2005). Position mapping on the mouse chromosome was performed with a Basic Local Alignment Search Tool (BLAST) search using the University of California Santa Cruz Genome Bioinformatics database (<http://genome.ucsc.edu>) and the definition of a CIS was the same as in the retrovirus tagged cancer gene database (<http://RTCGD.ncicrf.gov>) (Akagi *et al.*, 2004).

Pathological and flow cytometric analyses

Smears and stamp specimens of leukemic tissues were examined as described (Honda *et al.*, 1999). Flow cytometric analysis were performed as previously described (Miyazaki *et al.*, 2009).

Colony assays

Colony assays were performed as previously described (Miyazaki *et al.*, 2009). In brief, 1×10^5 BM cells were subjected for a B-cell colony formation assay using MethoCult M3630 (StemCell Technologies, Inc., Vancouver, Canada), which contains 10 ng/ml rhIL-7. After 12–14 days of incubation, colony numbers were counted.

Conflict of interest

The authors declare no conflict of interest.

Acknowledgements

We thank Yuki Sakai, Kayoko Hashimoto, Yuko Tsukawaki and Rika Tai, for the care of the mice and technical assistance, Dr Nobuaki Yoshida for E14 ES cells, Dr Søren Warming, Dr

Neal G Copeland and Dr Nancy A Jenkins for mouse *Zfp521* cDNA, Dr Koichi Ikuta for mouse *TCRJB* probe, Dr Hiroataka Matsui for statistical analysis and Dr Takuro Nakamura for helpful discussion. This work was in part supported by a grant-in-aid from the Ministry of Education, Science and Culture of Japan, a grant-in-aid for Cancer Research from the Ministry of Health, Labour and Welfare of Japan (13-2), Takeda Science Foundation, Astellas Foundation for Research on Metabolic Disorders, the Japan Leukaemia Research Fund and Tsuchiya Foundation.

Authorship

Contribution: NY, Z-iH, TI and HH designed and performed the research and wrote the paper; HO centralized the pathological analysis; RK and LW generated the retrovirus; KM, MM and TS participated in the flow cytometric analysis; AN performed colony assays. All the authors checked the final version of the paper.

References

- Akagi K, Suzuki T, Stephens RM, Jenkins NA, Copeland NG. (2004). RTCGD: retroviral tagged cancer gene database. *Nucleic Acids Res* 32: (Database issue) D523–527.
- Aspland SE, Bendall HH, Murre C. (2001). The role of E2A-PBX1 in leukemogenesis. *Oncogene* 20: 5708–5717.
- Bain G, Engel I, Robanus Maandag EC, te Riele HP, Voland JR, Sharp LL *et al.* (1997). E2A deficiency leads to abnormalities in alphabeta T-cell development and to rapid development of T-cell lymphomas. *Mol Cell Biol* 17: 4782–4791.
- Bain G, Maandag EC, Izon DJ, Amsen D, Kruisbeek AM, Weintraub BC *et al.* (1994). E2A proteins are required for proper B cell development and initiation of immunoglobulin gene rearrangements. *Cell* 79: 885–892.
- Beverly LJ, Capobianco AJ. (2003). Perturbation of Ikaros isoform selection by MLV integration is a cooperative event in Notch(IC)-induced T cell leukemogenesis. *Cancer Cell* 3: 551–564.
- Bond HM, Mesuraca M, Amodio N, Mega T, Agosti V, Fanello D *et al.* (2008). Early hematopoietic zinc finger protein-zinc finger protein 521: a candidate regulator of diverse immature cells. *Int J Biochem Cell Biol* 40: 848–854.
- Dang J, Inukai T, Kurosawa H, Goi K, Inaba T, Lenny NT *et al.* (2001). The E2A-HLF oncoprotein activates Groucho-related genes and suppresses Runx1. *Mol Cell Biol* 21: 5935–5945.
- Gilks CB, Bear SE, Grimes HL, Tschlis PN. (1993). Progression of interleukin-2 (IL-2)-dependent rat T cell lymphoma lines to IL-2-independent growth following activation of a gene (Gfi-1) encoding a novel zinc finger protein. *Mol Cell Biol* 13: 1759–1768.
- Hentges KE, Weiser KC, Schountz T, Woodward LS, Morse HC, Justice MJ. (2005). Evi3, a zinc-finger protein related to EBFAZ, regulates EBF activity in B-cell leukemia. *Oncogene* 24: 1220–1230.
- Higuchi M, O'Brien D, Kumaravelu P, Lenny N, Yeoh EJ, Downing JR. (2002). Expression of a conditional AML1-ETO oncogene bypasses embryonic lethality and establishes a murine model of human t(8;21) acute myeloid leukemia. *Cancer Cell* 1: 63–74.
- Honda H, Fujii T, Takatoku M, Mano H, Witte ON, Yazaki Y *et al.* (1995). Expression of p210bcr/abl by metallothionein promoter induced T-cell leukemia in transgenic mice. *Blood* 85: 2853–2861.
- Honda H, Inaba T, Suzuki T, Oda H, Ebihara Y, Tsujii K *et al.* (1999). Expression of E2A-HLF chimeric protein induced T-cell apoptosis, B-cell maturation arrest, and development of acute lymphoblastic leukemia. *Blood* 93: 2780–2790.
- Hunger SP. (1996). Chromosomal translocations involving the E2A gene in acute lymphoblastic leukemia: clinical features and molecular pathogenesis. *Blood* 87: 1211–1224.
- Inaba T, Inukai T, Yoshihara T, Seyschab H, Ashmun RA, Canman CE *et al.* (1996). Reversal of apoptosis by the leukaemia-associated E2A-HLF chimaeric transcription factor. *Nature* 382: 541–544.
- Inaba T, Roberts WM, Shapiro LH, Jolly KW, Raimondi SC, Smith SD *et al.* (1992). Fusion of the leucine zipper gene HLF to the E2A gene in human acute B-lineage leukemia. *Science* 257: 531–534.
- Inukai T, Inaba T, Yoshihara T, Look AT. (1997). Cell transformation mediated by homodimeric E2A-HLF transcription factors. *Mol Cell Biol* 17: 1417–1424.
- Inukai T, Inoue A, Kurosawa H, Goi K, Shinjo T, Ozawa K *et al.* (1999). SLUG, a ces-1-related zinc finger transcription factor gene with antiapoptotic activity, is a downstream target of the E2A-HLF oncoprotein. *Mol Cell* 4: 343–352.
- Jonkers J, Berns A. (1996). Retroviral insertional mutagenesis as a strategy to identify cancer genes. *Biochem Biophys Acta* 1287: 29–57.
- Kuhn R, Schwenk F, Aguet M, Rajewsky K. (1995). Inducible gene targeting in mice. *Science* 269: 1427–1429.
- Kurosawa H, Goi K, Inukai T, Inaba T, Chang KS, Shinjo T *et al.* (1999). Two candidate downstream target genes for E2A-HLF. *Blood* 93: 321–332.
- Lin H, Grosschedl R. (1995). Failure of B-cell differentiation in mice lacking the transcription factor EBF. *Nature* 376: 263–267.
- Look AT. (1997). Oncogenic transcription factors in the human acute leukemias. *Science* 278: 1059–1064.
- Matsunaga T, Inaba T, Matsui H, Okuya M, Miyajima A, Inukai T *et al.* (2003). Regulation of annexin II by cytokine-initiated signaling pathways and E2A-HLF oncoprotein. *Blood* 103: 3185–3191.
- Mikkers H, Berns A. (2003). Retroviral insertional mutagenesis: tagging cancer pathways. *Adv Cancer Res* 88: 53–99.
- Miyazaki K, Kawamoto T, Tanimoto K, Nishiyama M, Honda H, Kato Y. (2002). Identification of functional hypoxia response elements in the promoter region of the DEC1 and DEC2 genes. *J Biol Chem* 277: 47014–47021.
- Miyazaki K, Yamasaki N, Oda H, Kuwata T, Kanno Y, Miyazaki M *et al.* (2009). Enhanced expression of p210BCR/ABL and aberrant expression of Zfp423/ZNF423 induce blast crisis of chronic myelogenous leukemia. *Blood* 113: 4702–4710.
- Mizuno T, Yamasaki N, Miyazaki K, Tazaki T, Koller R, Oda H *et al.* (2008). Overexpression/enhanced kinase activity of BCR/ABL and altered expression of Notch1 induced acute leukemia in p210BCR/ABL transgenic mice. *Oncogene* 27: 3465–3474.
- Nakamura T. (2005). Retroviral insertional mutagenesis identifies oncogene cooperation. *Cancer Sci* 96: 7–12.

- Nakayama H, Ishimaru F, Avitah N, Sezaki N, Fujii N, Nakase K et al. (1999). Decreases in Ikaros activity correlate with blast crisis in patients with chronic myelogenous leukemia. *Cancer Res* **59**: 3931–3934.
- Rosenbaum H, Harris AW, Bath ML, McNeill J, Webb E, Adams JM et al. (1990). An E mu-v-abl transgene elicits plasmacytomas in concert with an activated myc gene. *EMBOJ* **9**: 897–905.
- Scheijen B, Jonkers J, Acton D, Berns A. (1997). Characterization of pal-1, a common proviral insertion site in murine leukemia virus-induced lymphomas of c-myc and Pim-1 transgenic mice. *J Virol* **71**: 9–16.
- Seidel MG, Look AT. (2001). E2A-HLF usurps control of evolutionarily conserved survival pathways. *Oncogene* **20**: 5718–5725.
- Shinto Y, Morimoto M, Katsumata M, Uchida A, Aozasa K, Okamoto M et al. (1995). Moloney murine leukemia virus infection accelerates lymphomagenesis in E mu-bcl-2 transgenic mice. *Oncogene* **11**: 1729–1736.
- Smith KS, Rhee JW, Cleary ML. (2002). Transformation of bone marrow B-cell progenitors by E2a-Hlf requires coexpression of Bcl-2. *Mol Cell Biol* **22**: 7678–7687.
- Smith KS, Rhee JW, Naumovski L, Cleary ML. (1999). Disrupted differentiation and oncogenic transformation of lymphoid progenitors in E2A-HLF transgenic mice. *Mol Cell Biol* **19**: 4443–4451.
- Wang J, Iwasaki H, Krivtsov A, Febbo PG, Thorner AR, Ernst P et al. (2005). Conditional MLL-CBP targets GMP and models therapy-related myeloproliferative disease. *EMBOJ* **24**: 368–381.
- Warming S, Liu P, Suzuki T, Akagi K, Lindtner S, Pavlakis GN et al. (2003). Evi3, a common retroviral integration site in murine B-cell lymphoma, encodes an EBFAZ-related Krüppel-like zinc finger protein. *Blood* **101**: 1934–1940.
- Wolff L, Garin MT, Koller R, Bies J, Liao W, Malumbres M et al. (2003a). Hypermethylation of the Ink4b locus in murine myeloid leukemia and increased susceptibility to leukemia in p15(Ink4b)-deficient mice. *Oncogene* **22**: 9265–9274.
- Wolff L, Koller R, Hu X, Anver MR. (2003b). A Moloney murine leukemia virus-based retrovirus with 4070A long terminal repeat sequences induces a high incidence of myeloid as well as lymphoid neoplasms. *J Virol* **77**: 4965–4971.
- Yamashita N, Osato M, Huang L, Yanagida M, Kogan SC, Iwasaki M et al. (2005). Haploinsufficiency of Runx1/AML1 promotes myeloid features and leukaemogenesis in BXH2 mice. *Br J Haematol* **131**: 495–507.
- Yoshihara T, Inaba T, Shapiro LH, Kato JY, Look AT. (1995). E2A-HLF-mediated cell transformation requires both the trans-activation domains of E2A and the leucine zipper dimerization domain of HLF. *Mol Cell Biol* **15**: 3247–3255.
- Zhuang Y, Soriano P, Weintraub H. (1994). The helix-loop-helix gene E2A is required for B cell formation. *Cell* **79**: 875–884.
- Zörnig M, Schmidt T, Karsunky H, Grzeschiczek A, Möröy T. (1996). Zinc finger protein GFI-1 cooperates with myc and pim-1 in T-cell lymphomagenesis by reducing the requirements for IL-2. *Oncogene* **12**: 1789–1801.

Supplementary Information accompanies the paper on the Oncogene website (<http://www.nature.com/onc>)

